The protective effect of homoplantaginin on AP cells is regulated by the circDNMT3B/miR-20b-5p/SLC7A11 axis through the modulation of ferroptosis

Shanfeng Sheng[1], Xiao Teng[1], Mingyuan Pan[2], Zhiquan Zhuang[1], Zhaohua Lin[1], Zheng Li[1,*]

[1]Wuming Hospital of Guangxi Medical University, Nanning, Guangxi, China

[2]The Second Affiliated Hospital of Guangxi Medical University, Nanning, Guangxi, China

Introduction. Acute pancreatitis (AP) is a common and potentially life-threatening inflammatory disease of the pancreas, with 20% of patients progressing to severe acute pancreatitis（SAP）, which is associated with a high mortality rate. Cellular ferroptosis has been implicated in the pathogenesis of AP; however, the specific mechanisms remain unclear. Objective: This study aims to elucidate the molecular mechanisms by which homoplantaginin（Hom）regulates ferroptosis in AP cells through the circDNMT3B/miR-20b-5p/SLC7A11 axis.

Methods. An in vitro model of AP was established using the mouse pancreatic acinar cell line 266-6, induced by caerulein. The biological characteristics of caerulein-treated 266-6 cells were assessed through Cell Counting Kit-8 (CCK-8) assays, flow cytometry, ELISA, qPCR, and Western blot analysis. The circDNMT3B inhibitor was transfected into cells to achieve gene knockdown of circDNMT3B, and the results were compared with those of the blank control group.

Results. In comparison with the blank control group, it was observed that the treatment with Hom resulted in a significant decrease in the levels of IL-1β, IL-18, MDA, PTGS2, and ACSL4 (all $p < 0.01$) as well as Fe^{2+} content and GSH (both $p < 0.05$) in the AP cells. Conversely, the expression levels of SLC7A11 and GPX4 were significantly elevated (both $p < 0.01$). It was further demonstrated that Hom treatment downregulated the expression of miR-20b-5p ($p < 0.01$) while upregulating the expression of circDNMT3B ($p < 0.001$) and Slc7a11 ($p < 0.01$). Additionally, it was found that the knockdown of the circDNMT3B gene led to a significant increase in the inflammatory levels of AP cells ($p < 0.05$), an elevation in

amylase content ($p < 0.01$), a reduction in apoptosis of AP cells ($p < 0.001$), and an enhancement of ferroptosis in the cells.

Conclusion. Hom is able to upregulate the expression of circDNMT3B and downregulate the expression of miR-20b-5p through the circDNMT3B/miR-20b-5p/SLC7A11 axis, thereby resulting in the increased expression of SLC7A11 and GPX4 in cells. This modulation is associated with the regulation of ferroptosis and a reduction in the inflammatory levels of acute pancreatitis. Furthermore, the circDNMT3B gene is suggested to play a protective role in the context of AP cell injury.

Keywords. homoplantaginin；acute pancreatitis；ferroptosis；SLC7A11；circDNMT3B

1. INTRODUCTION

Acute pancreatitis (AP) can progress to severe acute pancreatitis (SAP) as the condition deteriorates. SAP is often characterized by transient organ dysfunction or the occurrence of systemic or local complications, with a mortality rate reaching 20-30%，and it is a common yet extremely dangerous acute abdominal condition[1]. Despite advancements in the multidisciplinary approach to the treatment of AP, including improved strategies and rationalized nursing and nutritional models, cases of progression from AP to SAP still occur. Although the mortality rate associated with SAP has decreased, it remains significantly high. Ferroptosis is a process of iron-dependent cell death characterized by the accumulation of iron and the disruption of iron homeostasis within cells, leading to the oxidation of polyunsaturated fatty acids on cellular membranes by reactive oxygen species, resulting in lipid peroxidation and subsequent cell membrane damage[2]. Ferroptosis has been shown to be involved in the development and progression of various conditions, including cardiovascular diseases[3], tumors[4], infectious diseases[5], and metabolic disorders[6]. Therefore, the regulation of ferroptosis may represent an important therapeutic target for pharmacological intervention in these diseases.

Although some studies have demonstrated a close association between the progression of AP and ferroptosis, it has been observed that ferroptosis exacerbates the

inflammatory response in pancreatitis. Inhibition of glutathione peroxidase 4 (GPX4)-mediated pyrophosphorylation and ferroptosis may alleviate the inflammatory necrosis associated with acute pancreatitis and related pulmonary injury[7]; however, the specific mechanisms of ferroptosis in the context of AP remain unclear. Solute carrier family 7 member 11 (SLC7A11) is a cystine/glutamate reverse transporter, and its expression has been shown to enhance the activity of the antioxidant enzyme GPX4 and to inhibit cellular ferroptosis[8]. Numerous studies have confirmed that SLC7A11 participates in the negative regulation of ferroptosis alongside GPX4, and inhibition of SLC7A11 can lead to ferroptosis in glioma cells[9]. homoplantaginin, a flavonoid compound extracted from the plant Litchi chinensis, exhibits various pharmacological effects, including anti-inflammatory, antioxidant, and anti-tumor activities, and has been shown to have therapeutic effects on various inflammatory diseases[10, 11]. Homoplantaginin（Hom） is capable of modulating insulin sensitivity in endothelial cells by reducing the expression of inflammatory cytokines. Furthermore, it can regulate palmitic acid-induced apoptosis in endothelial cells, decrease the synthesis of nitric oxide, and inhibit the activation of NLRP3 and TLR4[12].

The role of miRNAs in AP has been widely recognized. For instance, it has been reported by Qin et al. that the expression levels of miR-22 and miR-135a are upregulated in acute edematous pancreatitis models[13]. It is suggested that miR-22 and miR-135a may promote the apoptosis of pancreatic acinar cells by inhibiting the expression of epidermal growth factor receptor 3 and protein tyrosine kinase 2 during acute edematous pancreatitis. In studies conducted by Zhang et al. on AP induced by rain frog toxin, it was discovered that miR-135a could mediate the apoptosis and inflammatory response of AR42J cells by targeting FAM129A[14]. Furthermore, research has confirmed that miR-21-3p regulates AP inflammation by upregulating the STAT3 protein inhibitor PIAS3 and downregulating HMGB1[15]. miR-20b-5p, a miRNA closely associated with various malignancies, is also implicated in the regulation of immune inflammatory responses. Circular RNA (circRNA) can act as

molecular sponges for miRNAs, thereby modulating the expression of relevant genes and pathway activation, which influences pancreatic cellular functions and participates in the development of AP. Bioinformatics analyses have shown that complementary bases exist between circDNMT3B and miR-20b-5p, and that a binding site for miR-20b-5p is also present in the 3' untranslated region of SLC7A11. Therefore, the objective of this study is to explore the inhibitory effects of Hom on pancreatic acinar cells in a mouse model of AP induced by rain frog toxin, through the regulation of the ferroptosis-related circDNMT3B/miR-20b-5p/SLC7A11 axis, aiming to provide a basis for clinical treatment of AP.

2. MATERIALS AND METHODS

2.1 Materials

2.1.1 Cell culture and modelling

The mouse pancreatic acinar carcinoma cell line 266-6 (specification: 1 × 10^6 cells) was purchased from Nanjing Zhongke Shikang Biotechnology Co., Ltd. The cells were cultured in DMEM medium supplemented with 10% FBS and 1% antibiotics, and were maintained in a humidified incubator at 37°C with 5% CO2. Passaging was performed every 2 to 3 days. Cells in the logarithmic phase of growth, which exhibited good growth conditions, were treated with 100 nmol/L of caerulein and cultured for 24 hours to establish the acinar pancreatic model.

2.1.2 Reagents and drugs

Special grade fetal bovine serum and DMEM medium were purchased from Gibco, USA; Streptomycin/Penicillin, CCK8 reagent, PMSF, Phosphatase Inhibitor, Annexin V-FITC/PI were purchased from Shanghai Biyuntian Reagent; ELISA kits of IL-1β, IL-6, IL-18, AMY, etc. were purchased from Shanghai Jianglai Bio-technology Co; DMSO, DEPC water, BCA protein quantification kit, GoldBand 3-colour Low Range Protein Marker, TRIzol, Hieff® qPCR SYBR Green Master Mix (High Rox Plus), Hifair® II 1st The GoldBand 3-colour Low Range Protein Marker, TRIzol, Hieff® qPCR SYBR Green Master Mix (High Rox Plus), Hifair® II 1st Strand cDNA

Synthesis SuperMix for qPCR (gDNA digester plus) were purchased from Next Sense Bio-Technology (Shanghai) Co Ltd, the GSH and MDA kits were purchased from Nanjing Zhongke Shikang Bio-Technology Co Ltd, and the 0.45uM PVDF membranes were purchased from MERCK (Germany).

2.2 Methods

2.2.1 Western blot

The cell samples were placed in 1.5 ml EP tubes, to which 1 ml of RIPA, 10ul of PMSF, and 20ul of phosphatase inhibitor were added, lysed at 4°C for 1 h, and centrifuged at 12,000 rpm for 5 min. The cell samples were subjected to BCA quantification (refer to the instructions of the YEASEN BCA Protein Quantification Kit). The expression levels of SLC7A11, GPX4, PTGS2, and ACSL4 were then measured.

2.2.2 CCK-8 assay

24h after transfection, 266-6 cells were implanted in 96-well plates at a density of 1000 cells/well and routinely cultured under the above conditions. Cell viability was measured at 24 h with CCK-8 reagent according to the manufacturer's protocol. The optical density (OD) value at 450 nm was measured by an enzyme marker (Bio-Rad, CA, USA).

2.2.3 Flow cytometric apoptosis

The apoptotic activity of mouse pancreatic alveolar 266-6 cells was calculated by Annexin V/FITC kit. Forty-eight hours after transfection, cells were collected into centrifuge tubes and centrifuged twice at 1000 rpm for 5 min, the supernatant was aspirated, and then resuspended by adding 1× binding buffer to adjust the cell density to 1-5×106/mL. 100 μL of cell suspension and 5 μL of Membrane Associated Protein V/FITC were then mixed, and the cells were incubated for 5 min at room temperature away from light. Before detection, 10 μL of propidium iodide (PI) and 400 μL of PBS were added.

2.2.4 ELISA test

Collect the cell supernatant and refer to Shanghai Jianglai ELISA kit instruction for

ELISA. Refer to Nanjing Jianglai GPX4, MDA biochemical kit instructions for detection.

2.2.5 RNA Extraction and Real-Time Quantitative PCR

One milliliter of Trizol was added to the cells and mixed thoroughly by pipetting, followed by incubation at 4°C for 15 minutes to ensure complete lysis. The solution was then transferred to a 1.5 ml centrifuge tube. Chloroform was added at a ratio of 200 µl per milliliter of Trizol, and the mixture was vigorously shaken for 30 seconds before being allowed to stand at 4°C for 15 minutes. The mixture was subsequently centrifuged at 4°C at 12,000 rpm for 15 minutes using a desktop centrifuge, allowing for complete phase separation. Four hundred microliters of the upper aqueous phase was carefully transferred to a sterile 1.5 ml RNase-free centrifuge tube, to which 400 µl of isopropanol was added. The solution was mixed and left at room temperature for 40 minutes to precipitate RNA. The solution was then centrifuged at 4°C at 12,000 rpm for 15 minutes, and the supernatant was discarded. Washing was performed twice with 1 ml of 75% ethanol, followed by centrifugation at 4°C at 12,000 rpm for 5 minutes, with the supernatant discarded each time. After the ethanol was evaporated in a clean bench, 30 µl of DEPC-treated water was added to dissolve the RNA, which was subsequently stored at -80°C for future use. The reaction system for quantitative PCR was prepared with a total volume of 20 µl. The primer sequences are indicated below:mmu_miR-20b-5p-F：5’-gcaaagtgctcatagtgcag-3’,

mmu_miR-20b-5p-R: 5’- gtccagttttttttttttttctacct-3’;

mmu_SLC7A11-F: 5’-CATCATCATCGGCACCGTCAT-3’,

mmu_SLC7A11-R: 5’-AGCAGTTCCACCCAGACTCGA-3’;

mmu_circ_DNMT3B-F: 5’-GACAAATCCCGTCTGCTTCC-3’,

mmu_circ_DNMT3B-R: 5’-GGTCTTCCAGATTGCCCTTGT-3’;

GAPDH-F: 5’- GCCAAAAGGGTCATCATCTCC-3’,

GAPDH-R: 5’- GTGATGGCATGGACTGTGGTC-3’;

U6-F: 5’- CTCGCTTCGGCAGCACA-3’,

U6-R: 5’- AACGCTTCACGAATTTGCGT-3’。

2.2.6 Cell Grouping and Treatment

To investigate the role of homoplantaginin in AP, four experimental groups were established: the blank control group, the AP group, the homoplantaginin (62.5 μmol/L) treatment group in AP, and the homoplantaginin (62.5 μmol/L) + RSL3 (5 μmol/L) treatment group in AP. For subsequent transfection experiments, three groups were designed: the caerulein-induced AP group, the homoplantaginin + siRNA-NC treatment group in AP, and the homoplantaginin + siRNA-circDNMT3B treatment group in AP.

2.2.7 Transfection

circDNMT3B inhibitor and negative control (NC) were purchased from Ribobio (Guangzhou, China). These fragments were then transfected into mouse pancreatic alveolar 266-6 cells by Lipofectamine 2000 (Invitrogen, Carlsbad, CA, USA) according to the manufacturer's procedures.

2.2.8 Statistical methods

Comparisons between samples of two groups were made using the independent samples t-test, one-way analysis of variance (ANOVA) test for multiple comparisons, and data were analysed using SPSS23.0 with at least three replications for each group, and GraphPad Prism 8.0 for graphing software. $P<0.05$ indicates that the difference is statistically significant.

3. RESULTS

3.1The inhibitory effect of homoplantaginin on caerulein-induced mouse pancreatic acinar cells was investigated

The in vitro AP cell model was established using mouse pancreatic acinar 266-6 cells treated with 100 nmol/L caerulein for 24 hours[16]. The results indicated that apoptosis levels were significantly reduced in the AP group ($p<0.001$, Figure 1A and C), while the homoplantaginin group and the homoplantaginin plus RSL3 intervention group exhibited a marked increase in apoptosis levels ($p<0.001$, Figure 1A and C). This suggests that caerulein-induced AP suppresses cell apoptosis and that

homoplantaginin can reverse the apoptosis suppression induced by caerulein, while the ferroptosis inducer RSL3 significantly increased apoptosis levels in AP cells. Both early and late stages of apoptosis induced by caerulein in AP displayed suppressed apoptosis levels ($p<0.001$, Figure 1B), while homoplantaginin reversed this suppression at both apoptotic stages ($p<0.01$, Figure 1B). Furthermore, the survival levels of AP cells treated with homoplantaginin and the ferroptosis inducer RSL3 were reduced ($p<0.001$, Figure 1B), indicating that ferroptosis promotes cell death in AP.

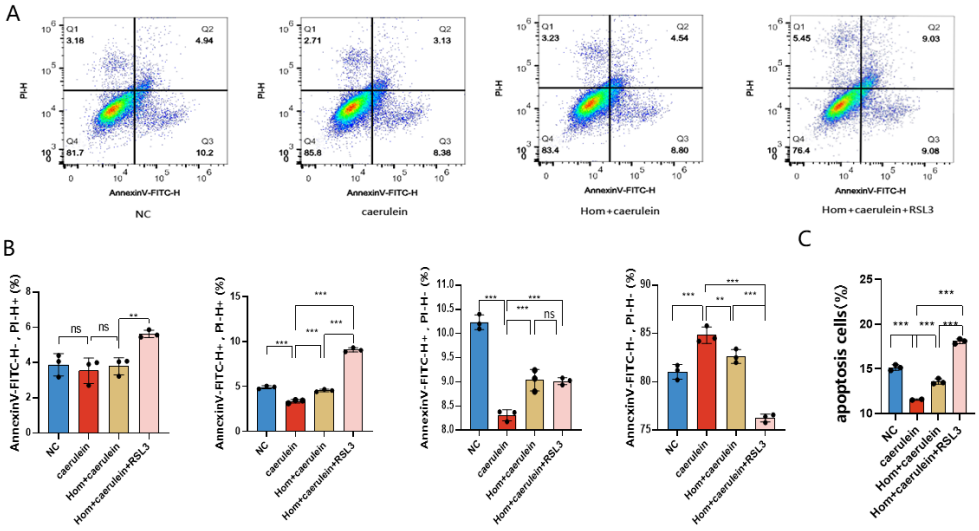

Figure.1 Modulation of apoptosis in AP cell model by homoplantaginin（The experiment was divided into four groups: a blank control group, a pancreatitis group induced by caerulein, a pancreatitis group treated with homoplantaginin, and a pancreatitis group treated with homoplantaginin in conjunction with RSL3. Figures 1A and 1B present the results of the flow cytometry analysis, while Figure 1C illustrates the survival rate of apoptotic cells. Statistical significance is indicated as follows: *$p < 0.05$, **$p < 0.01$, ***$p < 0.001$, with "ns" denoting non-significant comparisons.）

The growth of mouse pancreatic acinar 266-6 cells was observed for 24 hours (as shown in Figure 2D). In comparison to the blank control group, the levels of IL-1β

and IL-18 in the mouse pancreatic acinar 266-6 cell group induced by caerulein were significantly elevated ($p<0.05$, Figures 2F and $p<0.05$, Figures 2G), indicating the successful establishment of an inflammatory environment in the in vitro AP model. MDA, a byproduct of lipid peroxidation associated with cellular ferroptosis, was found to be significantly increased alongside the accumulation of Fe^{2+}, which is recognized as a hallmark of ferroptosis. The level of Fe^{2+} in the cells of the caerulein-induced AP group was elevated ($p<0.001$, Figure 2H), while both GSH and MDA levels were also significantly increased ($p<0.001$, Figures 2I and $p<0.05$, Figures 2J). This suggests that the occurrence and progression of AP induced by caerulein are closely related to cellular ferroptosis, which may facilitate the development of AP. In contrast to the AP group, the intervention with homoplantaginin significantly reduced the levels of IL-1β, IL-18, Fe^{2+}, GSH, and MDA in the AP group cells ($p<0.001$, Figures 2F, $p<0.001$, Figures 2G, $p<0.05$, Figures 2H, $p<0.05$, Figures 2I and $p<0.01$, Figures 2J). It is possible that this regulation of ferroptosis contributes to the reduction of inflammation in AP. Furthermore, in the homoplantaginin + RSL3 intervention AP group, compared to the homoplantaginin-only intervention AP group, the levels of Fe^{2+} and MDA were significantly increased ($p<0.001$, Figures 2H and $p<0.01$, Figures 2J), while the inflammatory markers did not show an increase.

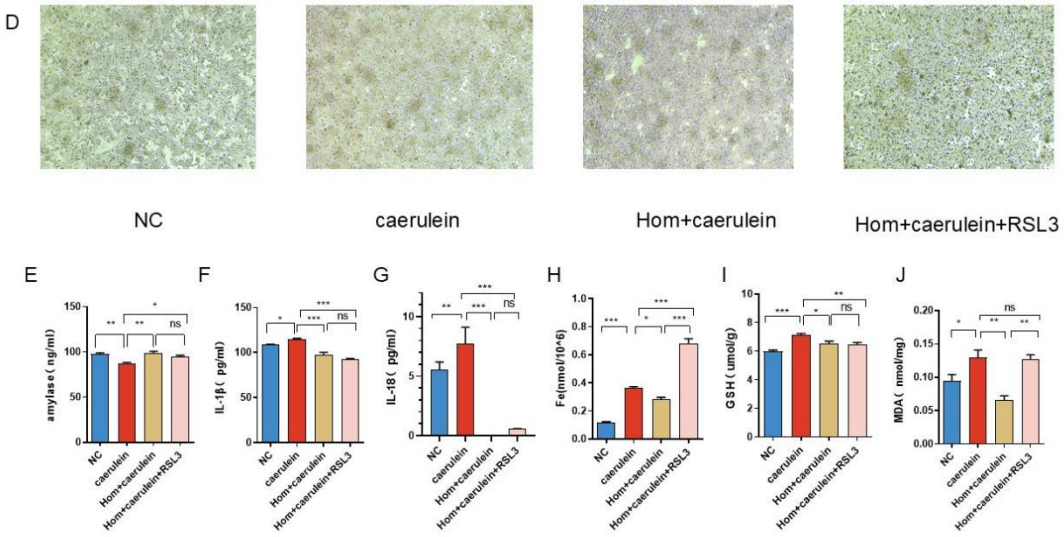

Figure.2 Inhibitory effect of homoplantaginin on caerulein-induced mouse pancreatic acinar cells（The experimental groups were consistent with those previously described. Figure 2D presents the growth profile of 266-6 cells at 24 hours (40× magnification). Figure 2E shows the detection of amylase in the cells, while Figures 2F and 2G illustrate the detection of IL-1β and IL-18 levels, respectively. Figure 2H depicts the measurement of cellular Fe^{2+} content, Figure 2I presents the assessment of GSH levels, and Figure 2J illustrates the detection of MDA in the cells. Statistical significance is indicated as follows: *p < 0.05, **p < 0.01, ***p < 0.001, with "ns" denoting non-significant comparisons.）

To further elucidate the regulatory effects of homoplantaginin on caerulein-induced ferroptosis in mouse pancreatic acinar cells, we used western blot to detect the expression levels of SLC7A11, GPX4, PTGS2, and ACSL4 in four groups of cells. The expression levels of SLC7A11 and GPX4 were significantly reduced in the caerulein-induced AP group ($p<0.05$, Figures 3B and C)), whereas the expression levels of PTGS2 and ACSL4 were significantly increased ($p<0.05$, Figures 3D and $p<0.01$, Figures 3E), which indicated that ferroptosis occurred in the caerulein-induced AP group. The expression levels of SLC7A11 and GPX4 were significantly increased in the homoplantaginin-treated AP group ($p<0.01$, Figures 3B and C), whereas the expression levels of PTGS2 and ACSL4 were significantly

decreased ($p<0.01$, Figures 3D and E), which indicated that homoplantaginin was able to regulate the ferroptosis of the AP cells, and further confirmed the assumption that homoplantaginin reduces the level of inflammation in the AP by regulating ferroptosis. Meanwhile, the expression levels of SLC7A11 and GPX4 were reduced in the homoplantaginin + RSL3-treated AP group compared to the homoplantaginin-intervened AP group ($p<0.01$, Figures 3B and C), whereas the expression levels of PTGS2 and ACSL4 were significantly increased ($p<0.01$, Figures 3D and E), which also confirmed that homoplantaginin was able to regulate the ferroptosis of AP cells.

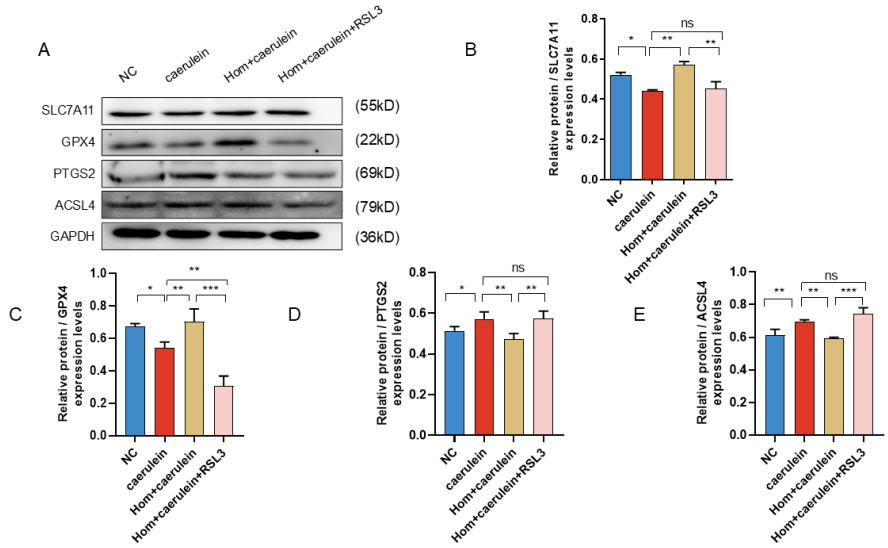

Figure.3 Homoplantaginin has the capacity to modulate ferroptosis in acute pancreatitis cells（The experimental groups were consistent with those previously described. Figures 3A, 3B, 3C, 3D, and 3E present the Western blot results for the expression levels of SLC7A11, GPX4, PTGS2, and ACSL4 in the cells. Statistical significance is indicated as follows: *$p < 0.05$, **$p < 0.01$, ***$p < 0.001$, with "ns" denoting non-significant comparisons.）

3.2 qPCR detection of cellular circDNMT3B, miR-20b-5p, *Slc7a11* expression

To investigate the specific regulatory mechanisms of homoplantaginin on the AP cell model, quantitative PCR (qPCR) was employed to measure the expression levels of circDNMT3B, miR-20b-5p, and *Slc7a11* in mouse pancreatic acinar 226-6 cells at 6 ,12 and 24 hours post-treatment. In the caerulein-induced AP group, the

expression level of miR-20b-5p was found to be elevated ($p<0.01$, Figure 4B), while the expression level of *Slc7a11* was decreased ($p<0.001$, Figure 4D). These findings suggest that the elevated inflammatory levels in the AP model may be associated with the increase in miR-20b-5p expression, while the reduction in *Slc7a11* expression indicates a diminished reverse transport of cystine and glutamate in the cells. In the homoplantaginin -treated AP group, a significant expression pattern of miR-20b-5p was observed, characterized by an initial increase followed by a decrease over time ($p<0.01$, Figure 4B). Additionally, the expression levels of circDNMT3B were significantly elevated at 6 and 24 hours ($p<0.001$, Figure 4C), and the expression levels of *Slc7a11* were markedly increased at 6 and 12 hours ($p<0.05$, Figure 4D). These results indicate that homoplantaginin can downregulate the expression of miR-20b-5p while simultaneously upregulating the expression of circDNMT3B and *Slc7a11*.

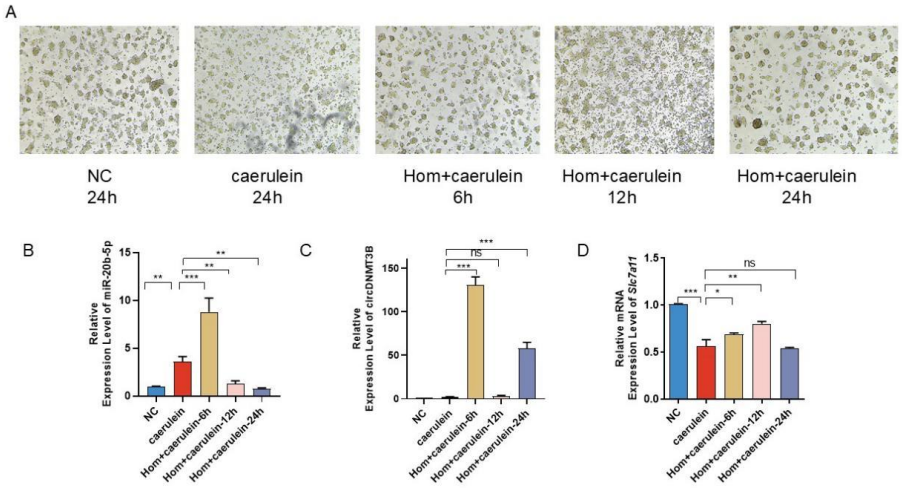

Figure.4 Homoplantaginin up-regulates the expression of circDNMT3B, Slc7a11 with down-regulation of miR-20b-5p （The experimental groups were consistent with those previously described. Figure 4A illustrates the growth profile of 266-6 cells at 6, 12, and 24 hours (40× magnification). Figures 4B, 4C, and 4D present the qPCR results for the expression levels of miR-20b-5p, circDNMT3B, and Slc7a11, respectively. Statistical significance is indicated as follows: *p < 0.05, **p < 0.01, ***p < 0.001, with "ns" denoting non-significant comparisons.）

3.3Homoplantaginin regulates the cellular circDNMT3B/miR-20b-5p/SLC7A11 axis to inhibit ferroptosis

To specifically investigate the biological effects of homoplantaginin on ferroptosis and inflammation in AP cells through the circDNMT3B/miR-20b-5p/SLC7A11 axis, we performed gene knockdown of the circDNMT3B gene in mouse pancreatic acinar 266-6 cells. In the pancreatitis group treated with homoplantaginin combined with siRNA-NC, there was a significant increase in cell apoptosis ($p < 0.001$, Figures 5A and 5B), along with a marked decrease in cell proliferation activity ($p<0.05$, Figure 5C). Additionally, the cellular amylase levels were reduced ($p<0.05$, Figure 5D), while the expression levels of the inflammatory factors IL-1β, IL-18, and IL-6 were elevate ($p<0.05$, Figures 5E, F, G). Notably, in the circDNMT3B knockdown AP group treated with homoplantaginin, apoptosis was reduced ($p<0.001$, Figure 5B), cell proliferation activity was significantly increased ($p<0.05$, Figure 5C), and amylase content was significantly elevated ($p<0.01$, Figure 5D), while the expression levels of inflammatory factors IL-1β and IL-6 increased significantly ($p<0.05$, Figures 5E, G). This suggests that circDNMT3B may play a protective role in AP, and the knockdown of circDNMT3B leads to increased inflammatory levels and the alleviation of apoptosis inhibition in AP. Subsequent studies revealed that in the AP group with circDNMT3B knockdown treated with homoplantaginin, the levels of Fe^{2+}, GSH, and MDA were significantly elevated ($p<0.001$, Figures 6H, I. $p<0.05$, Figures 6J). Concurrently, qPCR analysis demonstrated that in the AP group with circDNMT3B knockdown treated with homoplantaginin, the expression levels of miR-20b-5p, circDNMT3B, and SLC7A11 were reduced ($p<0.001$, Figures 6K, $p<0.01$, Figures 6L and $p<0.05$, Figures 6M). This suggests that circDNMT3B knockdown cells may induce ferroptosis and increase inflammation in AP cells through the regulation of the circDNMT3B/miR-20b-5p/SLC7A11 axis. Western blot analysis further revealed that the expression levels of SLC7A11 and GPX4 were decreased ($p<0.05$, Figures 6O, P), while the expression levels of PTGS2 and ACSL4 were elevated ($p<0.05$, Figures 6Q, R), confirming the occurrence of ferroptosis in AP cells.

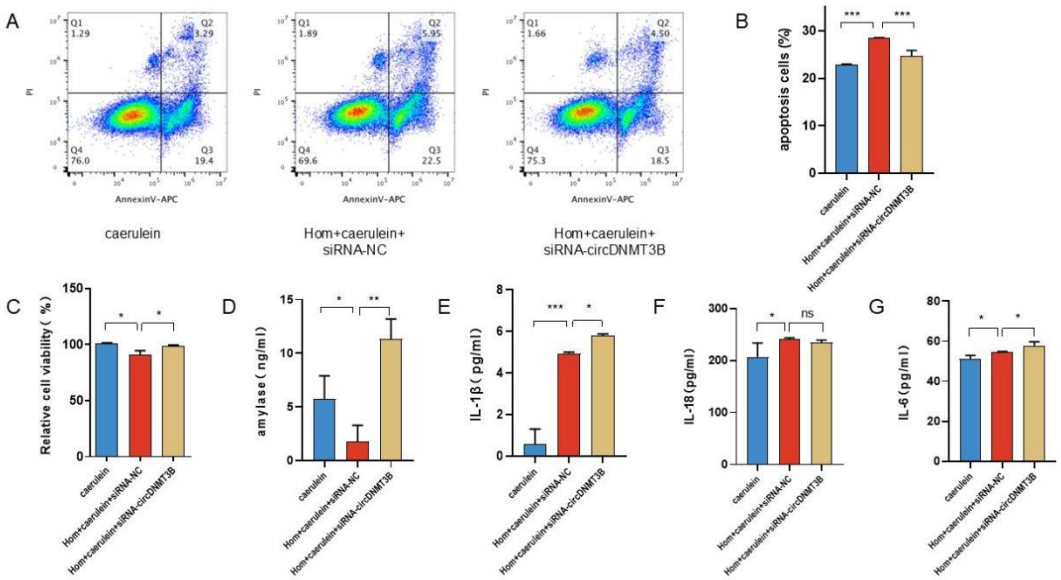

Figure.5 The knockdown of circDNMT3B enhances the inflammatory levels and apoptosis in AP cells

（The experiment was divided into three groups: a pancreatitis group induced by caerulein, a pancreatitis group treated with homoplantaginin combined with siRNA-NC, and a pancreatitis group treated with homoplantaginin combined with siRNA-circDNMT3B. Figures 5A and 5B present the results of the flow cytometry analysis, while Figure 5C shows the results of the CCK-8 assay. Figures 5D, 5E, 5F, and 5G depict the biochemical measurements of amylase, IL-1β, IL-18, and IL-6, respectively. Statistical significance is indicated as follows: *p < 0.05, **p < 0.01, ***p < 0.001, with "ns" denoting non-significant comparisons.）

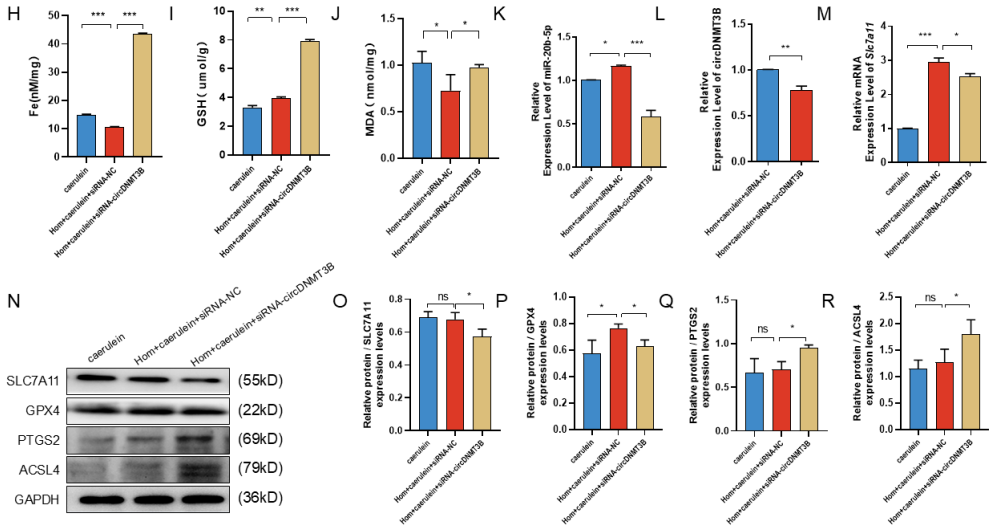

Figure.6 The knockdown of circDNMT3B promotes ferroptosis in AP cells

（The experiment was divided into three groups: a pancreatitis group induced by caerulein, a pancreatitis group treated with homoplantaginin combined with siRNA-NC, and a pancreatitis group treated with homoplantaginin combined with siRNA-circDNMT3B. Figures 6H, 6I, and 6J present the detection results for cellular Fe^{2+}, GSH, and MDA, respectively. Figures 6K, 6L, and 6M illustrate the qPCR results for the expression levels of miR-20b-5p, circDNMT3B, and Slc7a11. Finally, Figures 6N, 6O, 6P, and 6Q depict the Western blot results for the expression of SLC7A11, GPX4, PTGS2, and ACSL4 in the cells. Statistical significance is indicated as follows: *p < 0.05, **p < 0.01, ***p < 0.001, with "ns" denoting non-significant comparisons.）

4. DISCUSSION

Acute pancreatitis is characterized as an inflammatory disease, with the common causes predominantly being gallstones or alcohol-related factors. Conservative treatment is often employed for AP; however, the lack of specific targeted therapies may be a principal reason for its high mortality rate[17]. This observation underscores the necessity for a more in-depth investigation into the clinical pathogenesis of AP. Numerous studies have indicated that the occurrence and progression of AP are closely associated with ferroptosis in pancreatic acinar cells[18, 19], and severe acute pancreatitis is frequently accompanied by damage or even failure of other organs, such as the lungs[20] and kidneys[21]. Nevertheless, the mechanisms by which ferroptosis facilitates the onset and progression of acute pancreatitis, and potentially leads to its severe form, remain poorly understood.

In this study, an in vitro model of acute pancreatitis was established using the 266-6 mouse pancreatic acinar cell line[22]. It was found that homoplantaginin could reverse the apoptosis-inhibiting effects induced by caerulein in acute pancreatitis, while the ferroptosis inducer RSL3 promoted cell death in AP cells. Apoptosis was shown to have a protective effect on pancreatic acinar cells, which correlated negatively with the severity of acute pancreatitis inflammation[23]. Furthermore, Hom was found to reduce the inflammatory response in caerulein-induced AP cells, suggesting that this anti-inflammatory effect may be mediated by the regulation of cellular ferroptosis. In

the caerulein-induced AP group, the expression levels of SLC7A11 and GPX4 were significantly reduced, while PTGS2 and ACSL4 expression were increased, indicating a decrease in antioxidant capacity and an increase in ferroptosis. However, Hom was shown to elevate the expression of SLC7A11 and GPX4, while decreasing the levels of IL-1β, IL-18, Fe^{2+}, MDA, PTGS2, and ACSL4. This suggests that Hom can mitigate inflammatory damage by modulating ferroptosis levels in AP cells.

Notably, the innovative findings of our research indicated that homoplantaginin could upregulate the expression of circDNMT3B and downregulate miR-20b-5p, leading to the upregulation of SLC7A11 and GPX4, thereby modulating ferroptosis and inflammation levels in acute pancreatitis. The expression of SLC7A11 was associated with the restoration of redox homeostasis and cell survival[24], as it protects cells from ferroptosis[25]. Furthermore, Hom was shown to regulate the proliferation activity of mouse pancreatic acinar cells post-caerulein treatment, suggesting a protective role against cell damage induced by caerulein. GPX4, a selenium-dependent enzyme relying on GSH[26], catalyzes the reduction of toxic lipid peroxides to non-toxic alcohols in mitochondria and cytoplasm[27], working in conjunction with SLC7A11 to combat ferroptosis within the cellular antioxidant system[28]. MDA, a product of lipid peroxidation, and PTGS2, a gene associated with ferroptosis[29], were found to have elevated expression levels, indicating the occurrence of ferroptosis. PTGS2 catalyzes the synthesis of prostaglandins, with increased activity leading to the production of lipid peroxides and resulting in iron-dependent programmed cell death[30].

The role of homoplantaginin in the antioxidant system has been demonstrated[31] , and it is capable of modulating the molecular mechanisms between circDNMT3B, miR-20b-5p, and SLC7A11. Through this modulation, Hom may reduce inflammation in AP cells and protect the cells from damage. It has been reported that homoplantaginin promote autophagy via the AMPK/TFEB pathway[32] , which alleviates endothelial cell apoptosis caused by hyperglycemia. The existence of complementary bases between circDNMT3B and miR-20b-5p has been established, with the latter identified as its target gene [33]. In this study, it was found that the

knockdown of circDNMT3B significantly reduced the level of apoptosis, while the levels of amylase, F^{e2+}, IL-1β, IL-6, MDA, PTGS2, and ACSL4 were markedly increased. In contrast, the expression of SLC7A11 and GPX4 was significantly decreased, indicating that the knockdown of circDNMT3B promotes the occurrence of ferroptosis in AP cells, which implies a protective role of circDNMT3B in AP. Furthermore, literature has confirmed that silencing circDNMT3B expression can exacerbate oxidative damage in septic rats and influence the levels of inflammatory factors in intestinal tissues[33] . Additionally, miR-20b-5p has been shown to regulate cell proliferation, differentiation, apoptosis, and angiogenesis[34, 35] .

The inflammatory response in acute pancreatitis is suggested to be positively correlated with miR-20b-5p, while a negative correlation with circDNMT3B is indicated. Studies conducted by researchers using rat models and in vitro models have demonstrated that miR-20b-5p can regulate autophagy by targeting AKT3, thereby inhibiting inflammation and apoptosis, which in turn suppresses the occurrence of severe acute pancreatitis[36]. In experiments where Hom inhibited caerulein-induced ferroptosis in AP cells, the expressions of circDNMT3B and SLC7A11 were found to be elevated, while the expression of miR-20b-5p was significantly decreased. This suggests a potential targeted regulatory relationship among the three, with circDNMT3B and SLC7A11 playing protective roles in caerulein-induced ferroptosis in acute pancreatitis, while miR-20b-5p appears to promote inflammatory processes in AP. Additionally, circDNMT3B may negatively regulate the expression of miR-20b-5p[37]. A limitation of this study is the use of mouse pancreatic acinar 266-6 cells as a model for acute pancreatitis, which may not adequately reflect the interplay and immune response between the pancreas and other organs during acute pancreatitis, nor the integrity of human pancreatic acinar cells. Therefore, the specific targeted relationships among miR-20b-5p, circDNMT3B, and SLC7A11 require further validation. Future research should include more in vivo experiments to confirm the regulatory mechanisms involved.

In summary, this study established an in vitro model of mouse pancreatic acinar cells

for acute pancreatitis and demonstrated that homoplantaginin can regulate the expression of circDNMT3B/miR-20b-5p genes. This regulation led to elevated expressions of SLC7A11 and GPX4 in the cells, thereby modulating cellular ferroptosis levels and exerting protective effects against damage to pancreatic acinar cells in the context of acute pancreatitis. Additionally, the knockdown of the circDNMT3B gene was found to be closely associated with ferroptosis in mouse pancreatic acinar cells. This finding may provide a novel perspective for the study of therapeutic strategies and the progression of ferroptosis in acute pancreatitis.

CONFLICT OF INTEREST

The authors of this manuscript declare that there are no conflicts of interest associated with this work.

AUTHOR CONTRIBUTION STATEMENT

Shanfeng Sheng was responsible for the experimental operations, implementation of the research process, drafting the manuscript, developing the manuscript framework, and conducting statistical analysis. Xiao Teng and Mingyuan Pan assisted with the experiments, verified the data, and created the figures. Zhiquan Zhuang and Zhaohua Lin were responsible for revising the paper, translating the paper and manuscript revisions. Zheng Li was responsible for the study design, provision of funding, formulation of writing strategies and overall guidance in the preparation of the article, including final approval of the manuscript.

FUNDING

Guangxi Natural Science Foundation（serial number：2023GXNSFAA026206）

REFERENCES

[1] BOXHOORN L, VOERMANS R P, BOUWENSE S A, et al. Acute pancreatitis [J]. Lancet, 2020, 396(10252): 726-34.

[2] PARK E, CHUNG S W. ROS-mediated autophagy increases intracellular iron levels and ferroptosis by ferritin and transferrin receptor regulation [J]. Cell Death Dis, 2019, 10(11): 822.

[3] MIYAMOTO H D, IKEDA M, IDE T, et al. Iron Overload via Heme Degradation in the Endoplasmic Reticulum Triggers Ferroptosis in Myocardial Ischemia-Reperfusion Injury [J]. JACC Basic Transl Sci, 2022, 7(8): 800-19.

[4] FRIEDMANN ANGELI J P, KRYSKO D V, CONRAD M. Ferroptosis at the crossroads of cancer-acquired drug resistance and immune evasion [J]. Nat Rev Cancer, 2019, 19(7): 405-14.

[5] PRONETH B, CONRAD M. Ferroptosis and necroinflammation, a yet poorly explored link [J]. Cell Death Differ, 2019, 26(1): 14-24.

[6] MASALDAN S, BUSH A I, DEVOS D, et al. Striking while the iron is hot: Iron metabolism and ferroptosis in neurodegeneration [J]. Free Radic Biol Med, 2019, 133: 221-33.

[7] FAN R, SUI J, DONG X, et al. Wedelolactone alleviates acute pancreatitis and associated lung injury via GPX4 mediated suppression of pyroptosis and ferroptosis [J]. Free Radic Biol Med, 2021, 173: 29-40.

[8] WANG X, WANG Y, HUANG D, et al. Astragaloside IV regulates the ferroptosis signaling pathway via the Nrf2/SLC7A11/GPX4 axis to inhibit PM2.5-mediated lung injury in mice [J]. Int Immunopharmacol, 2022, 112: 109186.

[9] WANG Z, DING Y, WANG X, et al. Pseudolaric acid B triggers ferroptosis in glioma cells via activation of Nox4 and inhibition of xCT [J]. Cancer Lett, 2018, 428: 21-33.

[10] CONG Y, WU S, HAN J, et al. Pharmacokinetics of homoplantaginin in rats following intravenous, peritoneal injection and oral administration [J]. J Pharm Biomed Anal, 2016, 129: 405-9.

[11] ZHU J X, GUO M X, ZHOU L, et al. Evaluation of the anti-inflammatory material basis of Lagotis brachystachya in HepG2 and THP-1 cells [J]. J Ethnopharmacol, 2024, 318(Pt B): 117055.

[12] HE B, ZHANG B, WU F, et al. Homoplantaginin Inhibits Palmitic Acid-induced Endothelial Cells Inflammation by Suppressing TLR4 and NLRP3 Inflammasome [J]. J Cardiovasc

Pharmacol, 2016, 67(1): 93-101.

[13] QIN T, FU Q, PAN Y F, et al. Expressions of miR-22 and miR-135a in acute pancreatitis [J]. J Huazhong Univ Sci Technolog Med Sci, 2014, 34(2): 225-33.

[14] ZHANG K K, YU S S, LI G Y, et al. miR-135a deficiency inhibits the AR42J cells damage in cerulein-induced acute pancreatitis through targeting FAM129A [J]. Pflugers Arch, 2019, 471(11-12): 1519-27.

[15] GANZ T, NEMETH E. Iron homeostasis in host defence and inflammation [J]. Nat Rev Immunol, 2015, 15(8): 500-10.

[16] LIU K, LIU J, ZOU B, et al. Trypsin-Mediated Sensitization to Ferroptosis Increases the Severity of Pancreatitis in Mice [J]. Cell Mol Gastroenterol Hepatol, 2022, 13(2): 483-500.

[17] LI H, LIN Y, ZHANG L, et al. Ferroptosis and its emerging roles in acute pancreatitis [J]. Chin Med J (Engl), 2022, 135(17): 2026-34.

[18] SU M, CHEN F, HAN D, et al. PRMT7-Dependent Transcriptional Activation of Hmgb2 Aggravates Severe Acute Pancreatitis by Promoting Acsl1-Induced Ferroptosis [J]. J Proteome Res, 2024, 23(3): 1075-87.

[19] MA D, LI C, JIANG P, et al. Inhibition of Ferroptosis Attenuates Acute Kidney Injury in Rats with Severe Acute Pancreatitis [J]. Dig Dis Sci, 2021, 66(2): 483-92.

[20] WANG Z, LI F, LIU J, et al. Intestinal Microbiota - An Unmissable Bridge to Severe Acute Pancreatitis-Associated Acute Lung Injury [J]. Front Immunol, 2022, 13: 913178.

[21] HU Q, YAO J, WU X, et al. Emodin attenuates severe acute pancreatitis-associated acute lung injury by suppressing pancreatic exosome-mediated alveolar macrophage activation [J]. Acta Pharm Sin B, 2022, 12(10): 3986-4003.

[22] HE Y, HU C, LIU S, et al. Anti-Inflammatory Effects and Molecular Mechanisms of Shenmai Injection in Treating Acute Pancreatitis: Network Pharmacology Analysis and Experimental Verification [J]. Drug Des Devel Ther, 2022, 16: 2479-95.

[23] LU G, TONG Z, DING Y, et al. Aspirin Protects against Acinar Cells Necrosis in Severe Acute Pancreatitis in Mice [J]. Biomed Res Int, 2016, 2016: 6089430.

[24] KOPPULA P, ZHANG Y, ZHUANG L, et al. Amino acid transporter SLC7A11/xCT at the crossroads of regulating redox homeostasis and nutrient dependency of cancer [J]. Cancer

Commun (Lond), 2018, 38(1): 12.

[25] STOCKWELL B R, JIANG X. The Chemistry and Biology of Ferroptosis [J]. Cell Chem Biol, 2020, 27(4): 365-75.

[26] LIANG D, FENG Y, ZANDKARIMI F, et al. Ferroptosis surveillance independent of GPX4 and differentially regulated by sex hormones [J]. Cell, 2023, 186(13): 2748-64.e22.

[27] BERSUKER K, HENDRICKS J M, LI Z, et al. The CoQ oxidoreductase FSP1 acts parallel to GPX4 to inhibit ferroptosis [J]. Nature, 2019, 575(7784): 688-92.

[28] FU C, WU Y, LIU S, et al. Rehmannioside A improves cognitive impairment and alleviates ferroptosis via activating PI3K/AKT/Nrf2 and SLC7A11/GPX4 signaling pathway after ischemia [J]. J Ethnopharmacol, 2022, 289: 115021.

[29] WANG D, LI X, JIAO D, et al. LCN2 secreted by tissue-infiltrating neutrophils induces the ferroptosis and wasting of adipose and muscle tissues in lung cancer cachexia [J]. J Hematol Oncol, 2023, 16(1): 30.

[30] JIANG L, KON N, LI T, et al. Ferroptosis as a p53-mediated activity during tumour suppression [J]. Nature, 2015, 520(7545): 57-62.

[31] MENG N, CHEN K, WANG Y, et al. Dihydrohomoplantagin and Homoplantaginin, Major Flavonoid Glycosides from Salvia plebeia R. Br. Inhibit oxLDL-Induced Endothelial Cell Injury and Restrict Atherosclerosis via Activating Nrf2 Anti-Oxidation Signal Pathway [J]. Molecules, 2022, 27(6).

[32] FAN L, ZHANG X, HUANG Y, et al. Homoplantaginin attenuates high glucose-induced vascular endothelial cell apoptosis through promoting autophagy via the AMPK/TFEB pathway [J]. Phytother Res, 2023, 37(7): 3025-41.

[33] LIU J, LIU Y, ZHANG L, et al. Down-regulation of circDMNT3B is conducive to intestinal mucosal permeability dysfunction of rats with sepsis via sponging miR-20b-5p [J]. J Cell Mol Med, 2020, 24(12): 6731-40.

[34] ZHANG D, YI Z, FU Y. Downregulation of miR-20b-5p facilitates Mycobacterium tuberculosis survival in RAW 264.7 macrophages via attenuating the cell apoptosis by Mcl-1 upregulation [J]. J Cell Biochem, 2019, 120(4): 5889-96.

[35] WANG X, LIN B, NIE L, et al. microRNA-20b contributes to high glucose-induced podocyte

apoptosis by targeting SIRT7 [J]. Mol Med Rep, 2017, 16(4): 5667-74.

[36] TANG G X, YANG M S, XIANG K M, et al. MiR-20b-5p modulates inflammation, apoptosis and angiogenesis in severe acute pancreatitis through autophagy by targeting AKT3 [J]. Autoimmunity, 2021, 54(7): 460-70.

[37] ZHU K, HU X, CHEN H, et al. Downregulation of circRNA DMNT3B contributes to diabetic retinal vascular dysfunction through targeting miR-20b-5p and BAMBI [J]. EBioMedicine, 2019, 49: 341-53.

Corresponding Author:
Zheng Li
Wuming Hospital of Guangxi Medical University, Nanning, Guangxi, China
E-mail: lizheng1717@126.com